DNA Damage Produced by Enediynes in the Human Phosphoglycerate Kinase Gene in Vivo: Esperamicin A1 as a Nucleosome Footprinting Agent†

Jinghai Xu, Jiongru Wu, and Peter C. Dedon*

Division of Toxicology, 56-786, Massachusetts Institute of Technology, 77 Massachusetts Avenue, Cambridge, Massachusetts 02139

Received October 9, 1997; Revised Manuscript Received November 26, 1997

ABSTRACT: We have used both conventional and a modified version of ligation-mediated polymerase chain reaction (LMPCR) to study the role of chromatin structure in the selection of DNA targets by three DNA-cleaving enediynes in whole cells. On the basis of previous studies of enediyne target selection in nucleosomes, we focused on nucleosomes present in the human X-linked phosphoglycerate kinase (PGK1) gene. Damage produced by esperamicin A1 in cells containing a transcriptionally inactive copy of the X-chromosome is reduced compared to that in naked DNA in two regions that encompass ∼130 and ∼150 base pairs upstream of the PGK1 gene. These sizes are consistent with nucleosome core DNA. Damage produced by esperamicin A1 in the transcriptionally active form of the gene, in which nucleosomes are not apparent, did not show such a pattern. Esperamicin C, an analogue of esperamicin A1 lacking an intercalating anthranilate moiety, and calicheamicin, both groove binders, were found to cleave DNA throughout the nucleosome core and linker. These results confirm hypotheses generated from studies in isolated chromatin and reconstituted nucleosomes and suggest that enediynes may prove useful as chromatin footprinting agents.

The packaging of DNA as chromatin in cells alters both its conformation and dynamics (reviewed in refs *1* and *2*). These perturbations introduce another level of complexity to the mechanisms by which DNA-damaging chemicals select their targets. To better understand how genomic organization affects target selection by genotoxins, we have compared the DNA damage produced by two enediynes, calicheamicin and esperamicin, in a single-copy human gene in vivo. The results confirm our previous hypotheses about enediyne target selection in nucleosomes (*3*−*5*).

The nucleosome is a basic element of chromatin structure (*1*) as well as a model for the effects of protein binding on DNA structure and dynamics. It consists of two regions, core and linker. The core is composed of ∼146 base pairs of DNA wrapped ∼1.8 times in a left-handed superhelix around four pairs of histone proteins, and the linker represents the 20−60 base pairs of DNA joining adjacent cores (*1, 2*). In addition to the bending-induced changes in DNA structure, the nucleosomal DNA is constrained in its dynamics by protein−DNA contacts. This constraint contributes to the reduced binding of intercalating agents to nucleosome core DNA (*6*−*9*).

The enediyne family of antitumor antibiotics presents a unique opportunity to study the relationship between drug structure and selection of DNA targets in chromatin. Enediynes are a structurally diverse group of molecules (Figure 1), yet they share a common mechanism for producing DNA damage: the aglycon core forms a diradical intermediate that abstracts deoxyribose hydrogen atoms when situated in the minor groove of DNA. The resulting damage consists of O_2-dependent single- and double-strand lesions (reviewed in refs *10* and *11*).

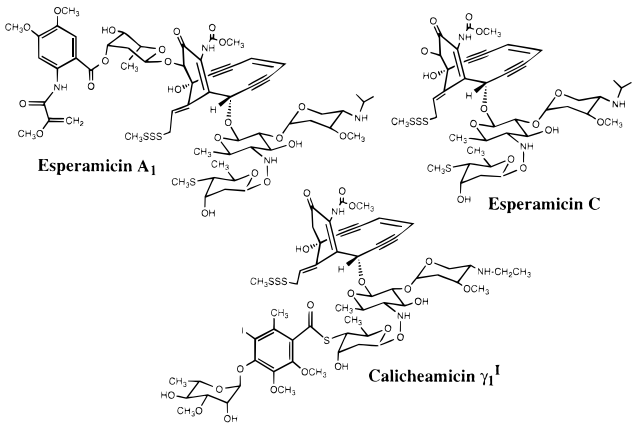

FIGURE 1: Structures of esperamicins A1 and C and calicheamicin γ_1I.

Despite this common mechanism, calicheamicin and esperamicin differ only in the organization of functional groups attached to the enediyne core (Figure 1). Specifically, the terminal carbohydrate−aromatic group of the calicheamicin tetrasaccharide side chain is positioned on the opposite side of the enediyne core in esperamicin A1, in the form of a deoxyfucose−anthranilate moiety. This group is missing in esperamicin C (Figure 1).

The diversity of enediyne structure suggested that the drugs would target different regions of chromatin in cells, a

† Supported by NIH/NCI Grant CA72936 (P.C.D.), the Samuel A. Goldblith Professorship (P.C.D.), and the Whitaker Health Sciences Fund Fellowship (J.X.).

* To whom correspondence should be addressed: Tel (617) 253-8017; Fax (617) 258-0225; E-mail pcdedon@mit.edu.

S0006-2960(97)02508-7 CCC: $15.00
Published on Web 01/30/1998

hypothesis supported by our studies in isolated chromatin (*4*) and reconstituted nucleosomes (*3, 5*). These studies revealed that esperamicin A1 was limited to damaging the linker region between nucleosome cores due to intercalation of an anthranilate moiety (*12*). However, calicheamicin and esperamicin C, which are nonintercalating groove-binders, damaged both the core and linker DNA (*3*−*5*); core DNA damage in this case was limited to sites where the minor groove faced away from the histone proteins. These observations serve as a model for the relationship between enediyne structure and in vivo target selection, and they suggest that the structural diversity of the enediynes can be exploited to probe chromatin structure in cells.

To test the validity of these in vitro models, we have now examined enediyne-induced damage in a single copy gene in living cells. Using ligation-mediated PCR (LMPCR), we demonstrate that esperamicin A1-induced DNA damage is suppressed in two putative nucleosome cores in the transcriptionally silent human phosphoglycerate kinase (PGK1) gene, while calicheamicin and esperamicin C produced damage throughout the nucleosome. We also observed that significantly higher drug concentrations were required to produce similar levels of damage in the inactive form of the PGK1 gene as in the active gene. These results suggest that enediynes may prove useful as chromatin footprinting agents.

MATERIALS AND METHODS

Materials and Cell Lines. Calicheamicin γ_1I and esperamicin A1 and C were provided by Dr. George Ellestad (Wyeth-Ayerst Research) and Dr. Jerzy Golik (Bristol-Myers Squibb), respectively. Chinese hamster−human hybrids containing either an inactive (cell line X86T2) or active human X chromosome (cell line Y162-11C) were provided by Dr. Stanley Gartler (University of Washington, Seattle, WA; *13*). A clone of X86T2 cells enriched in the human X chromosome was provided by Dr. Gerd Pfeifer (City of Hope Medical Center, Duarte, CA). Cells were grown as a monolayer in RPMI 1640 with 10% fetal calf serum and 40 μg/mL gentamicin (*13*). A clone of the upstream region of the human PGK1 gene, pBSHPGK1, was provided by Dr. Judith Singer-Sam (City of Hope Medical Center, Duarte, CA; *14*).

Treatment of Cells with Enediynes. Cells were harvested and resuspended in phosphate-buffered saline (PBS) at 10^7 cells/mL. An aliquot of calicheamicin or esperamicin in methanol was added (final methanol concentration <1%), and the reaction was allowed to proceed for 30 min at 37 °C. This incubation time was long enough to ensure that DNA damage was virtually complete (data not shown) yet short enough to avoid significant repair or apoptosis (*4*). We have previously demonstrated that enediyne-mediated DNA damage in nuclei is a direct result of the drug and is not mediated by topoisomerases or nucleases (*4*). The drug-damaged DNA was purified using a QiaAmp blood kit (Qiagen) and then treated with 100 mM putrescine for 1 h at 37 °C to cleave abasic sites (*15*−*17*). DNA samples were finally ethanol-precipitated and redissolved in 1 mM Tris and 0.1 mM EDTA (pH 7.8) at 1 mg/mL.

Treatment of Purified DNA with Enediynes. Genomic DNA was purified using a QiaAmp blood kit and dissolved in 50 mM HEPES, 5 mM EDTA, and 10 mM glutathione (pH 7.0) at 0.1 mg/mL. An aliquot of calicheamicin or esperamicin in methanol was added (final methanol concentration <1%), and the reaction was allowed to proceed for 30 min at 37 °C. The drug-damaged DNA was treated with putrescine as described above. DNA samples were then ethanol-precipitated and redissolved in 1 mM Tris and 0.1 mM EDTA (pH 7.8) at 1 mg/mL.

For DNA sequencing reactions, purified genomic DNA was concentrated by ethanol precipitation to 5−10 mg/mL. Maxam−Gilbert sequencing reactions were performed according to an LMPCR-optimized protocol (*18*).

LMPCR. We employed two LMPCR techniques that used the following primers in the 5′ region of the human PGK1 gene: CGTCCAGCTTGTCCAGC (+134 to +118, primer 1); TCCAGCGTCAGCTTGTTAGAAAGCG (+123 to +99, primer 2); TGGGGAGAGAGGTCGGTGATTCGGTCA (+80 to +54, primer 3); TCCAGCGTCAGCTTGTTAGAAAGCGACAT (+123 to +95, primer 4). The sequences of the blunt linker and linker primer were as described elsewhere (*19*). For conventional LMPCR (described in ref *20*), first-strand synthesis was performed with primer 1 and T7 DNA polymerase (Sequenase version 2.0, Amersham), followed by ligation with the blunt linker and T4 DNA ligase (Promega). PCR was performed with primer 2 and *Thermus aquaticus (Taq)* DNA polymerase (Boehringer Mannheim). Half of each sample was resolved on a 6% sequencing gel. Electroblotting and hybridization were performed as described elsewhere (*20*). The hybridization probe was made by repeated primer extension from a cloned PGK1 template (pBSHPGK1) using primer 3 and *Taq* polymerase (*21*). Hybridized membranes were subjected to phosphorimager analysis (Molecular Dynamics).

An alternative LMPCR strategy exploited the unique three-nucleotide 3′-overhangs present on all double-strand breaks produced by calicheamicin and esperamicins A1 and C (*12*, *22*). Drug-damaged DNA was ligated directly to a modified linker possessing a three-nucleotide 3′-overhang complementary to the drug-induced overhang. The modified linker consisted of a 28-mer oligonucleotide (GCGGTGACCCGGGAGATCTGAATTCNNN, where N represents a randomized nucleotide) annealed to an 11-mer oligonucleotide (5′-GAATTCAGATC) at 20 pmol/μL. Randomization of the three terminal nucleotides of the 28-mer was achieved using an equimolar mixture of all four nucleotides during synthesis (Oligos Etc.). The resulting population of oligonucleotides provided complementary 3′-overhangs for all possible damage sites. The use of the modified linker obviated the need for first-strand synthesis. Ligation reactions consisted of 2 μg of DNA, 7.5 μL of 10× ligase buffer (Promega), 1 μL of ligase (Promega, 3 units/μL), 100 pmol of modified linker, and sufficient water to yield a 75 μL final volume. Ligation was allowed to occur at 18 °C for 16 h. PCR amplification with primer 2 and linker primer was as described elsewhere (*20*). At the end of 20 cycles of amplification, each sample was transferred to ice and 5 μL of labeling mix was added; labeling mix contained 1 μL of 5× Taq buffer [200 mM NaCl, 50 mM Tris-HCl, pH 8.9, and 0.05% (w/v) gelatin], 2.5 pmol of the 5′-[^{32}P] end-labeled primer 4, 6.25 nmol of each dNTP, 1.5 units of *Taq* polymerase, and sufficient water to yield a 5 μL final volume (*23*). Amplification products

were then labeled by 2−4 repetitions of the following thermocycler program: 95 °C for 1 min, 69 °C for 2 min, and 76 °C for 10 min (*23*). Half of each sample was resolved on a 4−6% sequencing gel, which was then dried and subjected to phosphorimager analysis (Molecular Dynamics).

Data Analysis. To compare damage frequency in isolated and cellular DNA, we performed the experiments with drug concentrations that produced similar levels of DNA damage in the two situations. This amounts to roughly a 10-fold higher concentration of drug for cells than for isolated DNA (e.g., Figure 2). The difference is likely due to factors such as accessibility of DNA in higher order chromatin structures, sequestration of the drug in lipid membranes in the cells, or deactivation of the drugs in the cytoplasm.

We then accounted for unavoidable differences in the levels of DNA damage in different DNA samples and for lane-to-lane variation in gel loading. To do this, we normalized the phosphorimager signal intensities in each lane so that damage in putative nucleosome linker regions was the same in both isolated and cellular DNA. For example, the signal intensities for damage produced by esperamicin A1 in cellular DNA (Figure 2, lane 5) were multiplied by a factor of 3 so that damage frequencies in the region ∼+20 to ∼+70 were the same in both naked and cellular DNA. In this case, the factor of 3 represents the average difference in signal intensity for four major peaks in this region in isolated and cellular DNA (see Figure 3).

The validity of the normalization process is illustrated by three points. First, the expectation of equivalent amounts of damage in the nucleosome linkers has firm foundations in our previous in vitro studies (*4, 5*). Second, normalization of the data to the linker peaks is used consistently in all of our studies to avoid any biases. In fact, as shown in Figure 3B, normalization to the "linker region" in the transcriptionally active PGK1 gene (+20 to +70) results, as expected, in comparable levels of damage throughout the gene in naked and cellular DNA, since there is no nucleosome core present to suppress esperamicin-mediated DNA damage. Finally, normalization of the data to either of the two linker regions in the inactive PGK1 gene, (i.e., +20 to +70 and around position −200 in Figure 3A) produces the same result.

RESULTS

Mapping Esperamicin-Induced DNA Damage in the PGK1 Gene by Modified LMPCR. In this experiment, a modified linker was ligated directly to the double-strand breaks produced by esperamicins A1 and C. In control experiments with calicheamicin, which produces double-stranded DNA breaks exclusively (*22*), the modified linker produced a damage pattern nearly identical with that observed with conventional LMPCR (data not shown). It should be noted that single-strand breaks produced by esperamicin A1 would not be detected using the modified linker.

The damage produced by esperamicins A1 and C in naked DNA and in cells containing either an inactive PGK1 or an active PGK1 is shown in the gel in Figure 2 and in the line graphs in Figure 3. Examination of Figure 2 reveals that 10−20-fold higher concentrations of esperamicins A1 and C were required to produce comparable amounts of DNA damage in cellular DNA compared to isolated DNA. This was the case for all of the enediynes and, as discussed earlier, it was likely due to factors such as sequestration of the drug in lipid membranes in the cells or deactivation of the drugs in the cytoplasm.

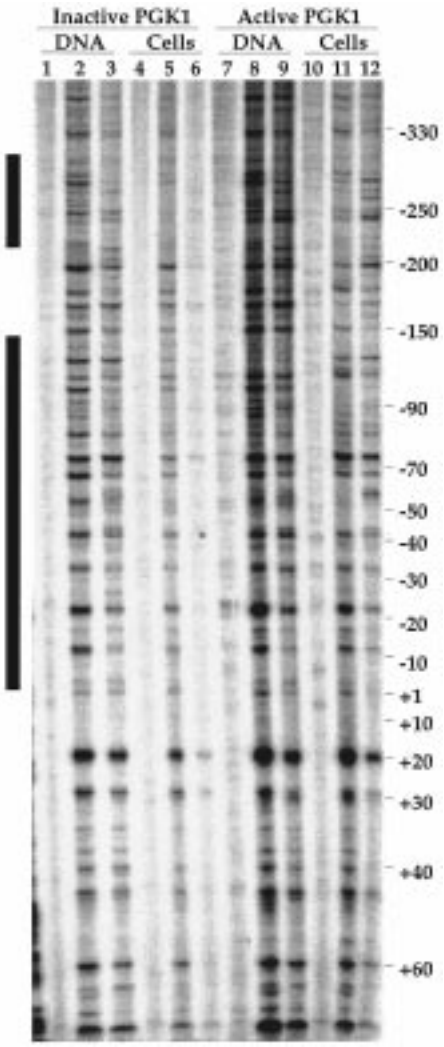

FIGURE 2: Sequencing gel analysis of the DNA damage produced by esperamicins in the inactive and active human PGK1 genes in vitro and in vivo. Modified LMPCR was employed to amplify sites of enediyne-induced strand breaks in the inactive PGK1 gene (X86T2 cells; lanes 1−6) and the active PGK1 gene (Y162-11C cells; lanes 7−12). Drug damage was studied in both isolated DNA (lanes 1−3 and 7−9) and in intact cells (lanes 4−6 and 10−12). Lanes 1, 4, 7, and 10, untreated controls; lanes 2 and 8, 0.1 μM esperamicin A1; lanes 5 and 11, 1 μM esperamicin A1; lanes 3 and 9, 0.1 μM esperamicin C; lanes 6 and 12, 1 μM esperamicin C. The amplified DNA was resolved on a 4% sequencing gel. The position in the PGK1 gene is shown in the right margin and the proposed positions of two nucleosomes are denoted by bars in the left margin. The weak cleavage apparent with esperamicin C in the inactive PGK1 gene in cells (lane 6) was due to a low drug concentration in this particular experiment; in other experiments with higher drug concentrations (10 μM), the damage was similar to that in isolated DNA (data not shown; e.g., Figure 4).

To address the role of the cellular environment of DNA in the damage produced by the enediynes, we have made quantitative comparisons of the various lanes in Figure 2 following normalization of the damage frequency data. In the inactive PGK1 gene, damage produced by esperamicin A1 in cells is reduced compared to that in naked DNA in two regions indicated by the bars in Figure 2. This

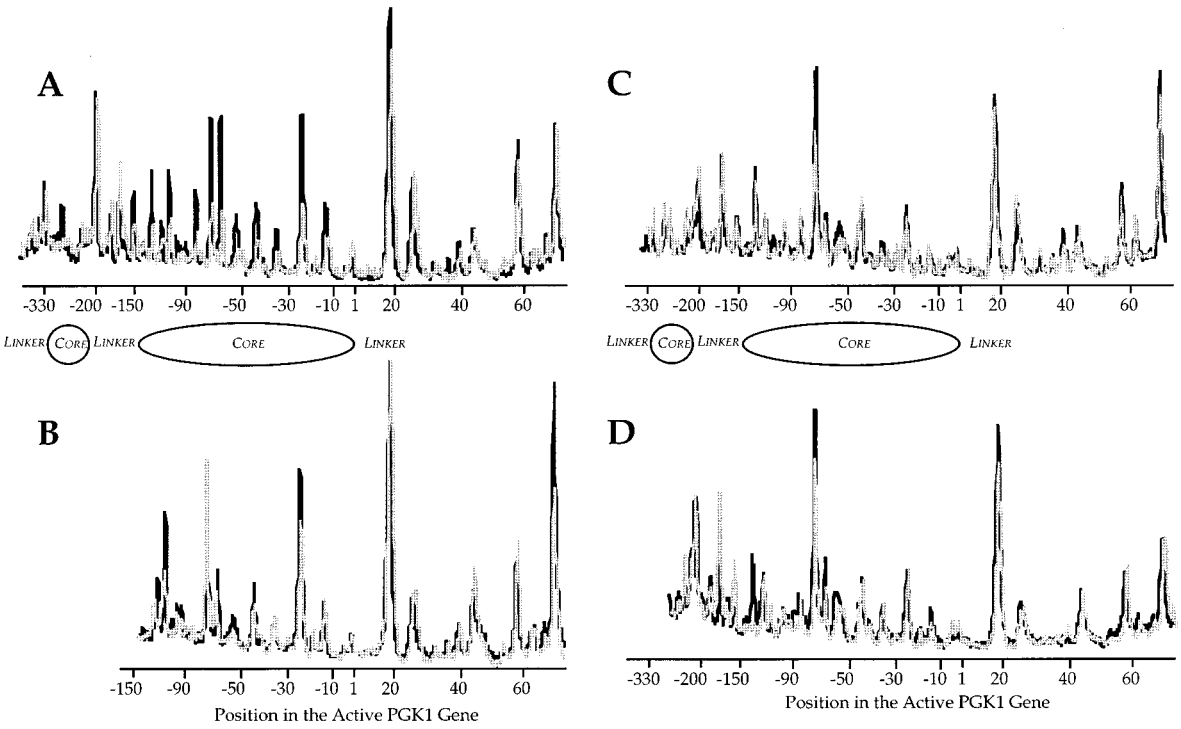

FIGURE 3: Comparison of DNA damage produced by esperamicin A1 (panels A and B) and esperamicin C (panels C and D) in the inactive (panels A and C) and active (panels B and D) human PGK1 gene. The gel shown in Figure 2 was subjected to phosphorimager analysis and the normalized data are presented as overlaid line graphs of damage frequency along the human PGK1 gene; the data displayed in panel C were derived from a different sequencing gel due to the low signal intensity of lane 6 in Figure 2. Black lines represent damage in isolated DNA and gray lines represent damage in cells. The position in the PGK1 gene is indicated below each graph and the proposed positions for two nucleosomes are indicated below the graph in panels A and C.

phenomenon is shown more clearly in Figure 3A, in which regions of reduced damage lie between positions −330 and −200 and between positions −150 and +1, and they are flanked by regions in which cellular and isolated DNA experience similar levels of damage. The sizes of the protected regions (∼130 and ∼150 base pairs) are consistent with the 146 base pair length of nucleosome core DNA (*1*). Furthermore, the identification of two nucleosomes in this region of the inactive PGK1 gene is consistent with the DNase I digestion studies of Pfeifer and Riggs (*24*).

Damage produced by esperamicin A1 in the transcriptionally active PGK1 gene contrasts with that in the inactive gene, as shown in the gel in Figure 2 and the line graphs in Figure 3B. When damage patterns in purified DNA and cells are compared, the two regions of damage suppression observed in the inactive genes are not apparent. These results are again consistent with the DNase I digestion studies of Pfeifer and Riggs, which suggest the absence of nucleosomes (*24*).

The profile of esperamicin C-induced DNA damage in the inactive PGK1 gene in cells is similar to that in isolated DNA (Figure 3C). There is no general reduction in the level of damage between positions −330 and −200 and between positions −150 and +1 as observed with esperamicin A1. Furthermore, the damage profiles for both the active and the inactive genes are quite similar (compare Figure 3 panels C and D).

Mapping Enediyne-Induced DNA Damage in the PGK1 Gene by Conventional LMPCR. Studies were also performed with conventional LMPCR to compare the in vivo and in vitro damage produced by enediynes, since this method recognizes both single- and double-strand breaks (*25*). Representative gels are shown in Figure 4 for esperamicins A1 and C and calicheamicin. As shown in the line graphs in Figure 5B,C, calicheamicin and esperamicin C produce damage in both the putative linker and core regions of the downstream nucleosome, while damage produced by esperamicin A1 occurs mainly outside the core DNA (Figure 5A).

There are several sites at which the damage frequency differs for isolated and cellular DNA treated with calicheamicin and esperamicin C. These sites may be located where the minor-groove faces the histone proteins, thus making the site inaccessible to the minor groove-specific enediynes. We have observed this phenomenon in isolated core particles (*4*) and reconstituted nucleosomes (*5*). However, many of the sites are subjected to similar levels of damage in both isolated and cellular DNA, which is consistent with damage at sites where the minor groove faces away from the histone proteins. Furthermore, there is no generalized suppression of the damage between positions −150 and +1 as observed with esperamicin A1.

The reproducibility of the results with both LMPCR techniques is demonstrated in Figures 3 and 5. The damage patterns produced by esperamicin A1 are similar in DNA isolated from both the X86T2 (inactive PGK1) and Y162-11C (active PGK1) cells (black lines in Figure 3A,B). The DNA is identical in sequence in both cell lines except that cytosines in all CpG dinucleotides in the inactive PGK1 gene are methylated while those in the active gene are not. This may explain the increase in esperamicin A1-induced DNA damage observed at two sites between positions −50 and −90 in DNA isolated from the inactive chromosome (black line in Figure 3A) compared to that from the active

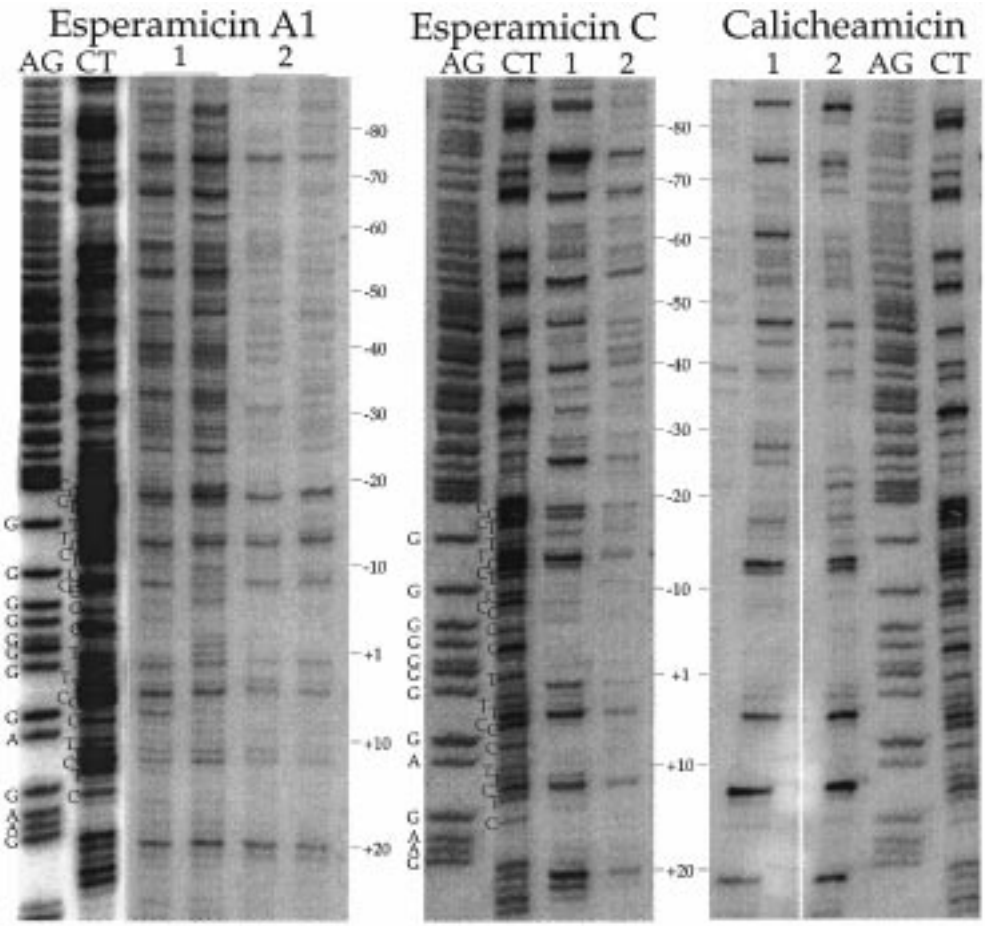

FIGURE 4: Sequencing gel analysis of the DNA damage produced by esperamicins A1 and C and calicheamicin in the inactive human PGK1 gene in vitro and in vivo. Conventional LMPCR was used to amplify sites of DNA damage produced by the enediynes in X86T2 cells (lane 2 in all panels) or in DNA isolated from these cells (lane 1 in all panels). Esperamicin A1 concentrations were 0.1 μM (in vitro, lane 1) and 1 μM (in vivo, lane 2); esperamicin C concentrations were 0.4 μM (in vitro, lane 1) and 10 μM (in vivo, lane 2); and calicheamicin concentrations were 0.1 μM (in vitro, lane 1) and 4 μM (in vivo, lane 2). The amplified DNA was resolved on a 6% sequencing gel. AG and CT are Maxam−Gilbert sequencing standards. The numbers on the right indicate the position in the human PGK1 gene. Please note that a lane to the right of the CT sequencing standard in the esperamicin A1 panel and a lane between the calicheamicin-treated samples were removed for clarity.

chromosome (black line in Figure 3B). We have previously observed that esperamicin-induced DNA damage is enhanced by cytosine methylation in DNA (*26*).

The reproducibility of the results is further demonstrated in Figures 4 and 5A. In Figure 4, duplicate samples of esperamicin A1-damaged isolated (lanes 1) and cellular DNA (lanes 2) are shown. While there are some minor bands that differ between the duplicate lanes, probably due to statistical sampling errors with low levels of damage (*25, 27*), the majority of bands are of similar intensity in each lane. Data beyond position −80 was not used for analysis due to unreliable amplification of long fragments by conventional LMPCR, as discussed later. Of greater importance, we have indicated the ratios of the level of esperamicin A1-induced DNA damage in cellular DNA to that in isolated DNA in Figure 5A. The damage ratio at each site is an average value (±SD) for three different experiments. The relatively small errors attest to the accuracy of the data.

DISCUSSION

The goal of the present work was to test the hypothesis that different enediynes would recognize different chromatin structures in living cells. This hypothesis arose from our previous studies in isolated chromatin (*4*) and reconstituted nucleosomes (*3, 5*), in which we observed that damage produced by esperamicin A1 was limited to the linker regions between nucleosome cores. The basis for this linker selectivity was determined to be intercalation by an anthranilate moiety (*12, 28*), which caused the drug to bind poorly to the dynamically constrained DNA of the nucleosome core. Consistent with this hypothesis was our observation that removal of the anthranilate to form esperamicin C caused the drug to damage both the core and linker DNA of the nucleosome. Furthermore, calicheamicin, another non-intercalating groove binder, was also capable of damaging both the core and linker DNA (*4, 5*). Subsequent studies revealed that calicheamicin preferentially targets curved or flexible DNA sequences (*29*).

The present results in whole cells confirm these in vitro observations. In the two nucleosome core-sized regions upstream of the inactive human PGK1 gene, damage produced by esperamicin A1, but not by esperamicin C and calicheamicin, is reduced in cells compared to naked DNA, while flanking regions (putative linkers) show similar levels of damage. One such region of suppressed damage lies between positions −330 and −200; the other, between −150

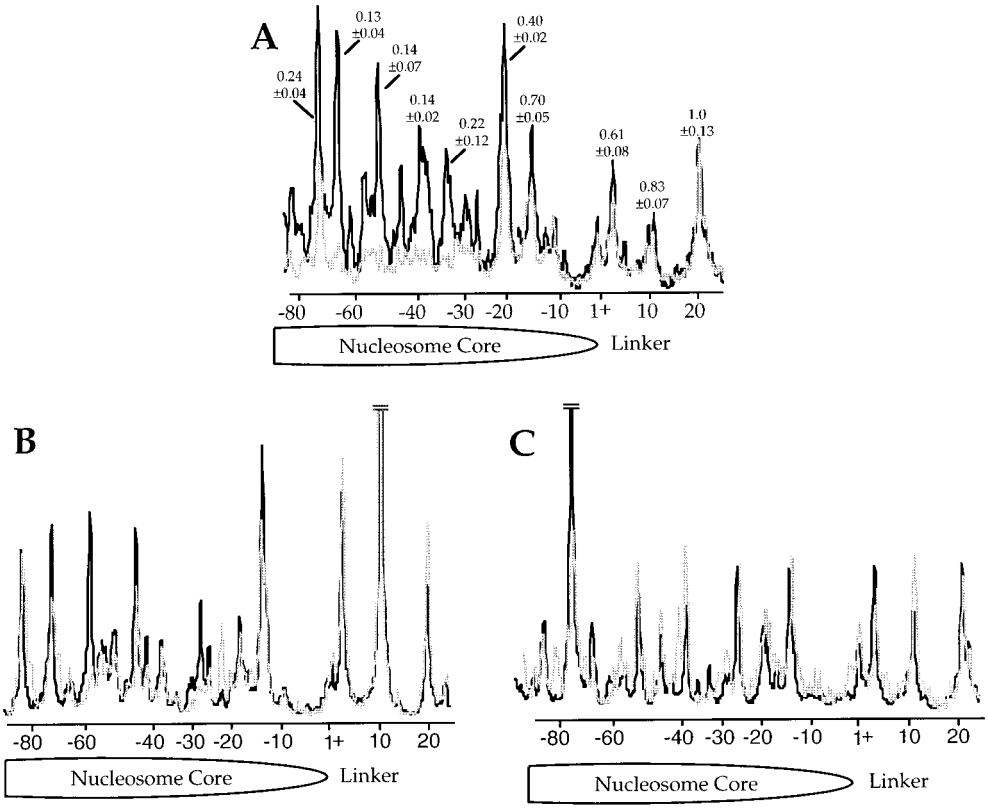

FIGURE 5: Comparison of DNA damage produced by esperamicin A1 (A), calicheamicin (B), and esperamicin C (C) in the inactive human PGK1 gene. The gels shown in Figure 4 were subjected to phosphorimager analysis and the normalized data are presented as overlaid line graphs of damage frequency along the human PGK1 gene. Black lines represent damage in isolated DNA and gray lines represent damage in cells. The numbers above the peaks in panel A represent the average ratios of the level of esperamicin A1-induced DNA damage in cellular DNA to that in isolated DNA at each site; the indicated errors are standard deviations for $n = 3$. The position in the PGK1 gene is noted below the graphs along with the proposed position of the nucleosome.

and +1. The two nucleosome cores would thus be joined by about 50 base pairs of linker DNA, which is typical for nucleosome linkers in mammalian cells (*1*). The second nucleosome core appears to end near position +1, as suggested by the results with both conventional and modified LMPCR (Figures 3 and 5).

The presence of two nucleosomes detected by esperamicin A1 in the inactive PGK1 gene and the absence of detectable nucleosomes in the active PGK1 gene are consistent with the nuclease digestion studies of Pfeifer and Riggs (*24*). They observed DNase I hypersensitive regions spaced at roughly 10 base pair intervals between positions −330 and −200 and between positions −90 and +50 in the inactive gene. However, this spacing would require a ∼110 base pair linker between the two nucleosomes, which is inconsistent with the observed linker sizes of ∼40−60 base pairs in vertebrate organisms and mammalian cells in culture (reviewed in ref *1*). There are at least two explanations for this discrepancy in the position of the downstream nucleosome. One is that detergent-induced disruption of the cell and nuclear membranes, which is required to allow entry of DNase I into the nucleus, causes sliding of the downstream nucleosome(s). Such sliding has been observed by several groups during nuclease digestions in isolated nuclei (reviewed in ref *1*). It is also possible that portions of the DNase I digestion pattern were influenced by factors other than accessibility of nucleosome core DNA, such as sequence selectivity of the enzyme or the presence of other chromosomal proteins. Confirmation of the nucleosome positions by micrococcal nuclease digestion was not possible in the studies of Pfeifer and Riggs, probably due to the fact that the region under study is very GC-rich and micrococcal nuclease shows a marked preference for AT-rich sequences (*24*).

In all of our studies, we observed low levels of esperamicin A1-induced damage in the nucleosome core DNA in vivo. This is likely due to transient disruption of nucleosomal structure during DNA replication and repair. Cells used in the present studies were monolayers at ∼80% confluency, so it is likely that some of the cells were in S-phase. While DNA transcription has also been shown to disrupt nucleosome structure (*30*), the X86T2 cells used in our studies contained only the inactive X chromosome. Thus the low levels of nucleosome core DNA cleavage by esperamicin A1 are not likely due to transcription.

We also observed that higher concentrations of the enediynes were required to produce levels of DNA damage in the inactive PGK1 gene that were similar to those in the active gene (Figure 2). This is consistent with the results of other studies with agents such as aflatoxin (*31*) and bleomycin (*32*), and it is likely due to a reduction in the accessibility of the DNA caused by higher order chromatin folding in transcriptionally silent DNA (reviewed in ref *1*). However, Zlatanova *et al*. have observed that methidium-propyl-EDTA, a linker-selective strand-cleaving intercalator (*33*), is not limited in its accessibility to certain regions of nucleosome-containing chromatin at varying degrees of salt-induced condensation (*34*). In light of our observations, salt-condensed chromatin may not be a good model for the

structure or environment of transcriptionally silent DNA in intact cells. It is also possible that a heterogeneity of condensed chromatin structures causes variable accessibility of DNA to small molecules and that our studies focus on a small, inaccessible region of the PGK1 gene.

It is noteworthy that, under our conditions, the LMPCR technique modified for enediyne-induced DNA damage consistently resulted in longer amplification products than conventional LMPCR. This allowed us to examine longer regions of the PGK1 gene for the location of drug-induced DNA breaks (compare Figures 3 and 5). The basis for this difference appears to lie in the use of Sequenase for the primer extension step of conventional LMPCR, since, in modified LMPCR, this step is eliminated by direct ligation of damage sites to the linker DNA; subsequent steps are identical in both techniques. Sequenase is a highly processive enzyme at 37 °C (*35*). However, first-strand synthesis was performed at 48 °C or above to reduce nonspecific amplification in conventional LMPCR (*36*) and it is possible that the elevated temperature reduced the processivity of the polymerase. Whatever the basis, LMPCR modified for enediyne-induced DNA damage allows longer regions of DNA to be examined on a single sequencing gel. The modified-linker technique is also applicable to the two-base-pair overhangs produced by other enediynes [e.g., C-1027 (*37, 38*)], as long as the ends of the linkers are changed to account for the different overhangs.

Enediynes offer several advantages over other methods for defining nucleosome positions. The main advantage is their utility with intact cells, since treatment of cells with enediynes does not disrupt the architecture of the cell or nucleus. The enediynes are lipophilic molecules that readily diffuse into cells. On the contrary, use of DNase I and micrococcal nuclease requires cell permeabilization to allow access of the enzymes to nuclear chromatin. In addition, DNase I-treated DNA often gives poor LMPCR signals due to polymerase extension from the enzyme-induced 3′ hydroxyl-ended strand breaks (*39*), and micrococcal nuclease is biased toward AT-rich regions (*24*). Methidiumpropyl-EDTA produces linker-selective DNA damage in isolated nuclei (*33*), though evidence is lacking for its utility in whole cells, and dimethyl sulfate, which readily penetrates the cell membrane, does not footprint nucleosomes (*40*). UV photofootprinting has the advantage of minimal cell perturbation and good sensitivity, but it is limited to the presence of dipyrimidines at the protein−DNA contact sites, and the need for additional DNA treatment by T4 endonuclease V and *Escherichia coli* photolyase (*41*). In comparison to these other agents, treatment of intact cells by enediynes is very straightforward and results in strand breaks with 5′-phosphate ends compatible with LMPCR.

In conclusion, we have found that esperamicin A1 can recognize locally positioned nucleosomes on the inactive human PGK1 gene in vivo, while esperamicin C and calicheamicin cleave both the core and linker DNA of the nucleosome. The results of these structure/function studies are consistent with in vitro models and serve as a benchmark for future explorations of the role of genomic organization in the selection of targets by enediynes and other genotoxins. The results also suggest that enediynes may prove useful as chromatin footprinting reagents.

ACKNOWLEDGMENT

We are grateful to Dr. Gerd Pfeifer for his advice and support in acquiring the LMPCR technology and for providing an X-chromosome-enriched clone of the X86T2 cells. Further thanks are extended to Dr. Stanley Gartler for providing the original hamster−human hybrid cells and to Dr. Judith Singer-Sam for providing the cloned PGK1 gene. We are also grateful to members of the Dedon laboratory for helpful discussions and critical reading of the manuscript.

REFERENCES

1. van Holde, K. E. (1989) *Chromatin*, Springer-Verlag: New York.
2. Wolffe, A. (1992) *Chromatin Structure and Function*, Academic Press, San Diego, CA.
3. Liang, Q., Choi, D.-J., & Dedon, P. C. (1998) *Biochemistry* (in press).
4. Yu, L., Goldberg, I. H., & Dedon, P. C. (1994) *J. Biol. Chem. 269*, 4144−4151.
5. Yu, L., Salzberg, A. A., & Dedon, P. C. (1995) *Bioorg. Med. Chem. 3*, 729−741.
6. Hurley, I., Osei-Gyimah, P., Archer, S., Scholes, C. P., & Lerman, L. S. (1982) *Biochemistry 21*, 4999−5009.
7. Chaires, J. B., Dattagupta, N., & Crothers, D. M. (1983) *Biochemistry 22*, 284−292.
8. McMurray, C. T., & van Holde, K. E. (1991) *Biochemistry 30*, 5631−5643.
9. McMurray, C. T., Small, E. W., & van Holde, K. E. (1991) *Biochemistry 30*, 5644−5652.
10. Dedon, P. C., & Goldberg, I. H. (1992) *Chem. Res. Toxicol. 5*, 311−332.
11. Lee, M. D., Ellestad, G. A., & Borders, D. B. (1991) *Acc. Chem. Res. 24*, 235−243.
12. Yu, L., Golik, J., Harrison, R., & Dedon, P. (1994) *J. Am. Chem. Soc. 116*, 9733−9738.
13. Hansen, R. S., Ellis, N. A., & Gartler, S. M. (1988) *Mol. Cell. Biol. 8*, 4692−4699.
14. Singer-Sam, J., Keith, D. H., Simmer, R. L., Shively, L., Lindsay, S., Yoshida, A., & Riggs, A. D. (1984) *Gene 32*, 409−417.
15. Lindahl, T., & Andersson, A. (1972) *Biochemistry 11*, 3618−3623.
16. Povirk, L. F., & Goldberg, I. H. (1985) *Proc. Natl. Acad. Sci. U.S.A. 82*, 3182−3186.
17. Dedon, P. C., & Goldberg, I. H. (1992) *Biochemistry 31*, 1909−1917.
18. Pfeifer, G. P., & Riggs, A. D. (1993) *Methods Mol. Biol. 23*, 169−181.
19. Mueller, P. R., & Wold, B. (1989) *Science 246*, 780−786.
20. Tornaletti, S., & Pfeifer, G. P. (1996) in *Technologies for Detection of DNA Damage and Mutations* (Pfeifer, G. P., Ed.) pp 199−209, Plenum Press: New York and London.
21. Sturzl, M., & Roth, W. K. (1990) *Anal. Biochem. 185*, 164−169.
22. Dedon, P. C., Salzberg, A. A., & Xu, J. (1993) *Biochemistry 32*, 3617−3622.
23. Mueller, P. R., & Wold, B. (1991) *Methods 2*, 20−31.
24. Pfeifer, G. D., & Riggs, A. D. (1991) *Genes Dev. 5*, 1102−1113.
25. Pfeifer, G. P., Steigerwald, S. D., Mueller, P. R., Wold, B., & Riggs, A. D. (1989) *Science 246*, 810−813.
26. Mathur, P., Xu, J., & Dedon, P. C. (1997) *Biochemistry 36*, 14868−14873.
27. Pfeifer, G. D., Drouin, R., & Holmquist, G. P. (1993) *Mutat. Res 288*, 39−46.
28. Ikemoto, N., Kumar, R. A., Dedon, P., Danishefsky, S. J., & Patel, D. J. (1994) *J. Am. Chem. Soc. 116*, 9387−9388.
29. Salzberg, A., Mathur, P., & Dedon, P. (1996) in *DNA and RNA Cleavers and Chemotherapy of Cancer and Viral*

Diseases (Meunier, B., Ed.), pp 23−36, Kluwer Academic Publishers, Dordrecht, The Netherlands.
30. Wolffe, A. P. (1994) *Regulation of chromatin structure and function*, R. G. Landes Company, Austin, TX.
31. Irvin, T. R., & Wogan, G. N. (1984) *Proc. Natl. Acad. Sci. U.S.A. 81*, 664−668.
32. Beckmann, R. P., Agostino, M. J., McHugh, M. M., Sigmund, R. D., & Beerman, T. A. (1987) *Biochemistry 26*, 5409−5415.
33. Cartwright, I. L., Hertzberg, R. P., Dervan, P. B., & Elgin, S. C. R. (1983) *Proc. Natl. Acad. Sci. U.S.A. 80*, 3213−3217.
34. Zlatanova, J., Leuba, S. H., Yang, G., Bustamente, C., & van Holde, K. (1994) *Proc. Natl. Acad. Sci. U.S.A. 91*, 5277−5280.
35. Tabor, S., & Richardson, C. C. (1989) *J. Biol. Chem. 264*, 6447−6458.
36. Rodriguez, H., Drouin, R., Holmquist, G. P., O'Connor, T. R., Boiteux, S., Laval, J., Doroshow, J. H., & Akman, S. A. (1995) *J. Biol. Chem. 270*, 17633−17640.
37. Xu, Y.-j., Zhen, Y.-s., & Goldberg, I. H. (1994) *Biochemistry 33*, 5947−5954.
38. Sugiura, Y., & Matsumoto, T. (1993) *Biochemistry 32*, 5548−5553.
39. Tormanen, V. T., Swiderski, P. M., Kaplan, B. E., Pfeifer, G. P., & Riggs, A. D. (1992) *Nucleic Acids Res. 20*, 5487−5488.
40. McGhee, J. D., & Felsenfeld, G. (1979) *Proc. Natl. Acad. Sci. U.S.A. 76*, 2133.
41. Pfeifer, G. P., Drouin, R., Riggs, A. D., & Holmquist, G. P. (1992) *Mol. Cell. Biol. 12*, 1798−1804.

BI972508T